Quantum Electronics **33** (1) 81 – 89 (2003)

INTERACTION OF LASER RADIATION WITH MATTER

PACS numbers: 47.10.+g, 61.30.-v
DOI: 10.1070/QE2003v033n01ABEH002368

Excitation of convective motions in isotropic and anisotropic liquids by light

R.S. Akopyan, R.B. Alaverdyan, L.Kh. Muradyan, G.E. Seferyan, Yu.S. Chilingaryan

Abstract. **The possibility of excitation of convective motions of the Rayleigh – Benard and Marangoni type in isotropic liquids and nematic liquid crystals upon absorption of light with a spatially periodic intensity distribution is demonstrated theoretically and experimentally. It is shown that gravitational and thermocapillary surface hydrodynamic waves are observed in the case of a running interference pattern. The possibility of control and the stability of convective motions are investigated. Benard cells become unstable when the light intensity is high. These instabilities are of thermal origin because the Prandtl number for the medium under investigation is considerably larger than unity. The competition between the gravitational and thermocapillary mechanisms of photohydrodynamic reorientation of the nematic liquid crystal director is also studied. The effect of convective motions on the thermodynamic phase transition is observed and explained.**

Keywords: *laser action, convection, instability, liquid crystals.*

1. Introduction

Convection in a layer of liquid heated from below is of considerable interest because convection is a simple example of motion caused by the ground-state instability. This instability appears when the Rayleigh number R characterising the equilibrium between the potential energy and the loss energy due to dissipation exceeds a certain critical value R_{cr}. Various aspects of stability of a horizontal layer of a liquid heated from below were investigated by many authors [1 – 3]. These effects are well known as the Rayleigh – Benard and Marangoni convective motions [4, 5]. An analysis of the peculiarities of thermal convection in nematic liquid crystals (NLCs) is of considerable importance because of their practical applications. It should be noted that instability thresholds in NLCs differ significantly from the instability threshold in isotropic liquids [6]. Unlike isotropic liquids, the NLC instability mechanism is governed by the director determining the direction of preferred orientation of molecules. As a result, steady-state convection occurs in a homotropically oriented NLC (whose molecules are oriented perpendicularly to the cell substrates) heated from above [7 – 9]. For example, Hopf bifurcation was observed in Ref. [9] in a homotropically oriented NLC in the case of Rayleigh – Benard convection.

The stability of regular convective motions is important in connection with the application of NLCs in applied physics problems. A transition from convective to absolute instability in a Hele – Shaw cell in the case of an unstable Kelvin – Helmholtz shift of the interface between two parallel flows of liquids was studied experimentally in [10].

The application of laser radiation makes it possible not only to achieve bulk heat release with almost any desirable spatial distribution, but also to control the parameters of this distribution. For example, the possibility of thermocapillary excitation of hydrodynamic motions by a laser beam was demonstrated experimentally for the first time in Refs [11 – 13], and the possibility of exciting regular convective motions in NLCs due to absorption of laser radiation with a spatially periodic intensity structure was predicted earlier in [14]. It was also shown that hydrodynamic flows lead to reorientation of the director and, hence, to a modulation of the permittivity of a NLC. The theory describing the strong orientation-convection-thermal nonlinearity predicted in Ref. [14] is given in [15].

The contribution of the above mechanism of optical nonlinearity to self-focussing of light in NLCs was observed for the first time in Ref. [16]. The NLC cell was closed on both sides so that only the gravitational mechanism of convection induced by the thermal expansion of the liquid was possible. Excitation of regular convective motions in an isotropic liquid with a single open surface was analysed theoretically [17] for the case when the liquid absorbed light with a spatially periodic structure of the intensity distribution. Convection was caused by the temperature dependence of the surface tension of the liquid (Marangoni thermocapillary mechanism). Forced convection and optical hydrodynamic reorientation of molecules in NLCs with a single free surface was investigated theoretically [18]. In the same paper, the competition between the gravitational and thermocapillary mechanisms was discussed and the conditions under which one of these mechanisms makes the main contribution to the convective motions were determined.

In this work, the gravitational and thermocapillary mechanisms of excitation of hydrodynamic convection in isotropic and anisotropic liquids, which is caused by

R.S. Akopyan, R.B. Alaverdyan, L.Kh. Muradyan, G.E. Seferyan, Yu.S. Chilingaryan Department of Physics, Yerevan State University, ul. Manukyana 1, 375025 Yerevan, Armenia;
e-mail: rhakob@yahoo.com

Received May 16, 2002
Kvantovaya Elektronika **33** (1) 81 – 89 (2003)
Translated by Ram Wadhwa

absorption of light with spatially periodic intensity distribution, were observed experimentally and studied theoretically. When a running periodic structure was produced, surface hydrodynamic waves were generated, whose propagation velocity coincided with the propagation velocity of the periodic structure. The stability of convective cells and surface hydrodynamic waves was studied and the possibility of the stability control was analysed.

2. Excitation of convective motions by a spatially periodic structure of a light wave

Consider a horizontal layer ($z = 0$, L) of a light-absorbing liquid or a liquid crystal with a free upper boundary ($z = L$) (Fig. 1). The layer is in the gravitational field with $\boldsymbol{g} = -g\boldsymbol{e}_z$ and absorbs light incident from above. We assume that two coherent plane light beams are incident on the free surface and form a spatially periodic pattern of the intensity distribution with period Λ. Weak absorption leads to a periodic heat release $Q = \alpha I_0[1 + \cos(kx)]$, where α is the light absorption coefficient; I_0 is the average total intensity of light; $k = 2\pi(\sin\alpha_1 - \sin\alpha_2)/\lambda$ is the wave number; α_1 and α_2 are the angles of incidence of the light beams on the liquid surface; and λ is the wavelength of light waves in vacuum.

We assume that heat is released symmetrically with respect to the coordinate y, so that $\partial/\partial y = 0$ and $v_y = 0$ ($\boldsymbol{v}$ is the velocity of hydrodynamic motions) everywhere. Hydrodynamic motions being excited are described by a system of equations of state, Navier–Stokes equations, and the equations of incompressibility and thermal conductivity for the hydrodynamic density ρ, pressure p, velocity $\boldsymbol{v}$, and temperature T. We write these variables in the form $T = T_0 + T'$, $p = p_0 + p'$, $\rho = \rho_0(1 - \beta T')$, where T_0, p_0, and ρ_0 are the unperturbed temperature, pressure ($p_0 = -\rho_0 g z + \text{const}$), and density; T', p', $\boldsymbol{v}$ are perturbations, and β is the volume expansion coefficient of the liquid. We will write the system of equations for the quantities T', p', $\boldsymbol{v}$ in the dimensionless form. A passage to dimensionless variables can be made in several ways. We will use the following most common procedure. We choose the layer thickness L as the unit of length, the time L^2/v of vertical thermal diffusion as the unit of time, χ/L as the unit of velocity, $\rho_0 v\chi/L^2$ as the unit of pressure, and $\alpha L^2 I_0/(\rho_0 c_p \chi)$ as the unit of temperature, where χ is the thermal diffusivity; $v = \eta/\rho_0$ is the kinematic viscosity; η is the viscosity coefficient; and c_p is the specific heat. In this case, the above-mentioned equations in the Boussinesq approximation can be written in the dimensionless form:

$$\frac{\partial \boldsymbol{v}}{\partial t} + \frac{1}{\mathrm{Pr}}(\boldsymbol{v}\nabla)\boldsymbol{v} = -\mathrm{grad}\, p + \Delta\boldsymbol{v} + \mathrm{R}T\boldsymbol{e}_z,$$

$$\mathrm{Pr}\frac{\partial T}{\partial t} + \boldsymbol{v}\nabla T = \Delta T + 1 + \cos(kx), \qquad (1)$$

$$\mathrm{div}\,\boldsymbol{v} = 0,$$

where $\mathrm{Pr} = v/\chi$ is the Prandtl number and $\mathrm{R} = g\beta I_0(\alpha L)L^4/(v\rho_0 c_p \chi^2)$ is the Rayleigh number for the heat source, which is associated with light absorption; for the sake of simplicity, we omit primes on the quantities. The equations for the z component of velocity and temperature in the steady-state regime of convective motions in the linear approximation have the form

$$\Delta\Delta v_{sz} + \mathrm{R}\Delta_\perp T_s = 0,$$
$$\Delta T_s + 1 + \cos(kx) = 0, \qquad (2)$$

where $\Delta_\perp = \partial^2/\partial x^2$. We assume that, at the rigid boundary $z = 0$, temperature T_0 is maintained and the boundary conditions for adhesion of the liquid are specified so that, for $z = 0$, we have

$$v_{sz}(x, z=0) = 0, \quad \left.\frac{\partial v_{sz}(x,z)}{\partial z}\right|_{z=0} = 0, \quad T_s(x, z=0) = 0. \qquad (3)$$

The boundary condition at the open surface $z = 1$ for the perturbation of temperature T_s correspond to linear heat removal in accordance with the Biot law [1] (we assume that heat removal is simply absent):

$$\left.\frac{\partial T_s}{\partial z}\right|_{z=1} = 0. \qquad (4)$$

The tangential force per unit area of the flat surface, which is associated with nonuniformity of the surface tension σ, is $\boldsymbol{f} = \nabla\sigma$; consequently, the boundary condition for the velocity taking into account the thermocapillary force can be written as

$$v_{sz}(x, z=1) = 0, \qquad \left.\frac{\partial^2 v_{sz}}{\partial z^2}\right|_{z=1} = \left.\frac{\mathrm{M}\partial^2 T_s}{\partial x^2}\right|_{z=1}, \qquad (5)$$

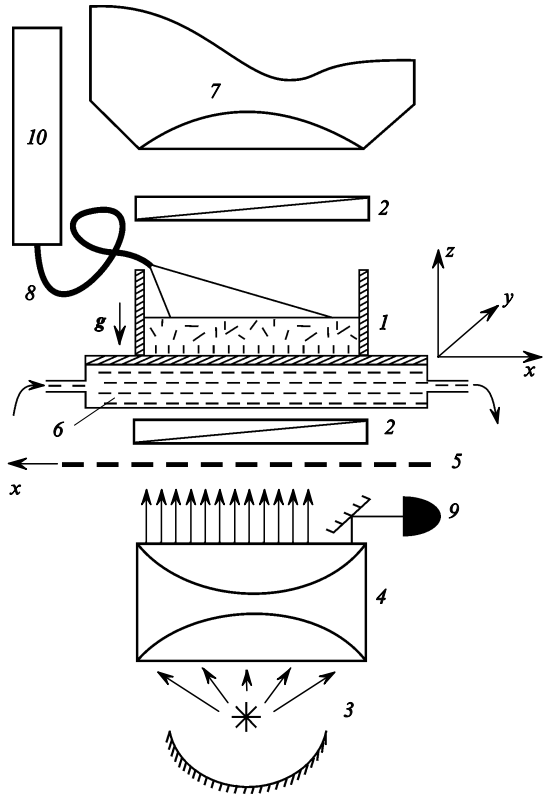

Figure 1. Schematic of the experimental setup: (*1*) cell with a liquid crystal; (*2*) polarisers; (*3*) light source (200-W halogen lamp); (*4*) condenser; (*5*) amplitude grating; (*6*) circulating water; (*7*) microscope; (*8*) optical fibre; (*9*) photodetector; (*10*) He–Ne laser.

where $M = \sigma_1(\alpha L)L^2 I_0/(\upsilon\chi^2\rho_0^2 c_p)$ is the Marangoni number and $\sigma_1 = -\partial\sigma/\partial T$. We must solve the system of equations (2) with the boundary conditions (3)–(5). The solution can be written in the form $v_{sz} = V(z)\cos(kx)$, $T_s = \theta_1(z) + \theta_2(z) \times \cos(kx)$.

The x component of the velocity can easily be measured in experiment. The boundary conditions for this component can be written in the form

$$v_{sx}(x, z=0) = 0, \quad \left.\frac{\partial v_{sx}}{\partial z}\right|_{z=1} = -\left.\frac{M\partial T_s}{\partial x}\right|_{z=1}. \tag{6}$$

The solution for the velocity component v_{sx} can be written as $v_{sx}(x,z) = -(1/k)(\partial V/\partial z)\sin(kx)$. Fig. 2 shows the dependence of the x and z velocity component on z. The calculations were made for the following parameters of the medium: $\rho_0 = 1.042$ g cm^{-3}, $\eta = 1.25$ P, $\chi = 10^{-4}$ cm^2 s^{-1}, $\beta = 5.3 \times 10^{-4}$ K^{-1}, $I_0 = 6$ W cm^{-2}, $\alpha = 50$ cm^{-1}, $L =$ 1 mm, $\rho c_p =$ 1 J cm^{-3} K^{-1}, $\sigma_1 = 10^{-2}$ dyne cm^{-1} K^{-1}, $R = 1.27 \times 10^5$, $M = 2.4 \times 10^5$.

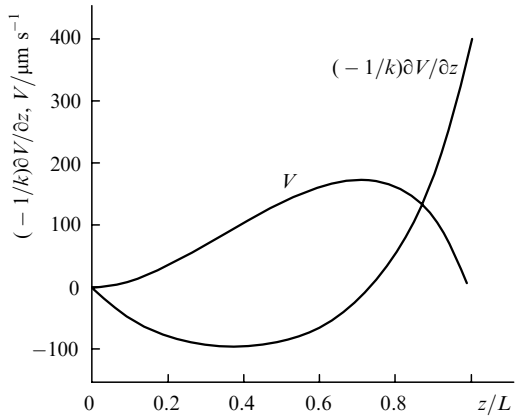

Figure 2. Dependences of the amplitudes of the x and z velocity components on the normalised coordinate z/L for the intensity $I_0 = 6$ W cm^{-2}, cell thickness $L = 1$ mm, and the period of intensity distribution $\Lambda = 2$ mm.

3. Excitation of hydrodynamic surface waves

Let two monochromatic waves with shifted frequencies ω_1 and ω_2 be incident on a horizontal layer of a liquid with the free surface $z = 0$, forming a running interference intensity pattern. In this case, the heat release can be written in a different form $Q = \alpha I_0[1 + 0.5\exp(ikx - i\omega t) + \text{c. c.}]$, where $\omega = \omega_1 - \omega_2$, and the experimental geometry is chosen so that the interference fringes are parallel to the y axis. The running interference pattern results in a running periodic heat release. The latter, in turn, leads to the appearance of convective rollers with the axes parallel to the direction of the interference fringes. These convective cylinders (rollers) move at right angles to this direction at a velocity ω/k.

In our analysis, it is important to take into account the z component of the velocity of the liquid $v_z(z=0) \neq 0$ on the free surface. The nonzero velocity exists because the assending regions of the liquid leave the plane $z = 0$ by inertia. This gives rise to the surface hydrodynamic waves of length $2\pi/k$ and velocity ω/k.

To solve the problem formulated above, we should modify the boundary conditions for $v_z(z=0)$. This can be done proceeding from the following considerations. First, the deformation of the free surface of the liquid generates the Laplace force $\sigma(\partial^2\xi/\partial x^2)$, where $\xi(x,t)$ is the displacement in the vertical direction from the unperturbed level of the surface $z = 0$. This force is balanced by the normal component of the viscous force σ_{zz} (σ_{ik} is the tensor of viscous stresses). Second, the tangential viscous forces are balanced by thermocapillary forces. The third boundary condition will be left unchanged (see Section 2). Thus, three boundary conditions for $z = 0$ can be written in the form

$$\sigma_{zz} = -p + 2\eta\frac{\partial v_z}{\partial z} = \sigma\frac{\partial^2\xi}{\partial x^2},$$
$$\sigma_{xz} = \sigma_{zx} = \eta\left(\frac{\partial v_x}{\partial z} + \frac{\partial v_z}{\partial x}\right) = \frac{\partial\sigma}{\partial x}, \qquad \frac{\partial T}{\partial z} = 0. \tag{7}$$

Considering that $v_z(z=0) = \partial\xi/\partial t$, we can write the solutions to the system of equations (1) (disregarding nonlinear terms) in the form

$$v_{x,z} = V_{x,z}(z)\exp(ikx - i\omega t) + \text{c. c.},$$
$$p = P(z)\exp(ikx - i\omega t) - \rho_0 gz + \text{c. c.}, \tag{8}$$
$$T = \Theta(z)\exp(ikx - i\omega t) + \text{c. c.}$$

By omitting the details of mathematical calculations, we write directly the expressions obtained for the temperature distribution on the liquid surface and the amplitude of capillary waves:

$$\Theta(z=0) = \frac{\alpha I_0}{\rho c_p(\chi k^2 - i\omega)}, \tag{9}$$

$$\xi = -i\frac{\sigma_1}{4\eta}\omega\frac{\Theta(z=0)}{gk + \sigma k^3/\rho - 2i\upsilon k^2\omega}\exp(ikx - i\omega t) + \text{c. c.} \tag{10}$$

In order to obtain numerical estimates, we use the values of parameters close to those typical of liquid crystals (e.g., MBBA) given in Section 2. Assuming, in addition, that $\sigma = 10$ dyne cm^{-1}, in the optical frequency range ($k \sim 10^2 - 10^5$ cm^{-1}), we obtain $\sigma k^3/\rho \sim 10^{18} - 10^{17}$. On the other hand, to excite surface waves, the displacement of the interference pattern should occur slower than the stabilisation of temperature and hydrodynamic velocity, i.e., $\omega \ll \chi k^2 \ll \upsilon k^2$. Under these conditions, expression (10) can be written in a simplified form:

$$\xi(x,t) = \frac{\sigma_1\omega\alpha I_0}{2\eta\sigma c_p\chi k^5}\sin(kx - \omega t). \tag{11}$$

To obtain a wave with amplitude $\xi = 1$ μm, the intensity of light waves must be $I_0 = 11.7$ W cm^{-2}; i.e., we deal with comparatively moderate powers. In this case, the maximum temperature of the medium is $\Theta_{max}(z=0) \approx 6.5 \times 10^3$ K, which is due to the absence of heat transfer. When the latter is taken into account, formula (9) is supplemented with the factor $1/[1 + b/(\chi k\rho c_p)]$, and the temperature of the liquid is two orders of magnitude lower (depending on the Biot number b).

Thus, an analysis of a semiinfinite light-absorbing liquid allows us to obtain a simple analytic solution of the problem in the form of a wave of the thermocapillary perturbation of the free surface of the liquid.

4. Stability of steady-state convective structures

Consider now the stability of steady-state convective Rayleigh – Benard cells. The stability of ordered convective structures for a fixed thickness of the cell depends strongly on the light intensity and on the period of an interference pattern.

Let the perturbed quantities in system (1) of dimensionless equations of thermal convection in the Boussinesq approximation have the form $\boldsymbol{v}_s + \boldsymbol{v}$, $p_s + p$, $T_s + T$. Below we will assume that $\mathrm{Pr} \gg 1$. In this case, we obtain the following scalar equations for $\boldsymbol{v}$, p, and T:

$$\begin{aligned} &\frac{\partial v_x}{\partial t} = -\frac{\partial p}{\partial x} + \Delta v_x, \\ &\frac{\partial v_z}{\partial t} = -\frac{\partial p}{\partial z} + \Delta v_z + \mathrm{R}T, \\ &\mathrm{Pr}\frac{\partial T}{\partial t} + v_{sx}\frac{\partial T}{\partial x} + v_{sz}\frac{\partial T}{\partial x} + v_x\frac{\partial T_s}{\partial x} + v_z\frac{\partial T_s}{\partial z} = \Delta T, \\ &\frac{\partial v_x}{\partial x} + \frac{\partial v_z}{\partial z} = 0. \end{aligned} \tag{12}$$

We now introduce the so-called stream function $\psi(x, z, t)$:

$$v_x = -\frac{\partial \psi}{\partial z}, \quad v_z = \frac{\partial \psi}{\partial x}. \tag{13}$$

Then, the equations for the stream function and temperature perturbation takes the form:

$$\begin{aligned} &\frac{\partial \Delta\psi}{\partial t} = \Delta\Delta\psi + \mathrm{R}\frac{\partial T}{\partial x}, \\ &\mathrm{Pr}\frac{\partial T}{\partial t} + v_{sx}\frac{\partial T}{\partial x} + v_{sz}\frac{\partial T}{\partial z} - \frac{\partial \psi}{\partial z}\frac{\partial T_s}{\partial x} + \frac{\partial \psi}{\partial x}\frac{\partial T_s}{\partial z} = \Delta T. \end{aligned} \tag{14}$$

We will seek the solutions to Eqns (14) in the form $\psi(x, z, t) = \alpha_0(z)\cos(kx)\exp(\gamma t)$, $T(x, z, t) = \Theta_0(z)\sin(kx)\exp(\gamma t)$, where γ is the logarithmic decrement of the stream function. Eliminating $T(x, z, t)$ from the system of equations and performing some transformations, we obtain the sixth-order differential equation for $\alpha_0(z)$:

$$\frac{\mathrm{d}^6\alpha_0}{\mathrm{d}z^6} - \left(3k^2 + \gamma\mathrm{Pr}\right)\frac{\mathrm{d}^4\alpha_0}{\mathrm{d}z^4} + \left(3k^4 + 2\gamma k^2\mathrm{Pr} + \gamma^2\mathrm{Pr}\right)\frac{\mathrm{d}^2\alpha_0}{\mathrm{d}z^2} - \left[k^6 + \gamma k^4\mathrm{Pr} + k^2\left(\gamma^2\mathrm{Pr} + \frac{1}{2}\mathrm{R}\right)\right]\alpha_0 = 0. \tag{15}$$

The boundary conditions for the amplitude $\alpha_0(z)$ of perturbations can be written in the form

$$\alpha_0(0) = 0, \quad \frac{\mathrm{d}\alpha_0(0)}{\mathrm{d}z} = 0, \quad \left[\frac{\mathrm{d}^4\alpha_0}{\mathrm{d}z^4} - \left(2k^2 + \gamma\right)\frac{\mathrm{d}^2\alpha_0}{\mathrm{d}z^2}\right]\Bigg|_{z=0} = 0,$$

$$\alpha_0(1) = 0, \quad \left[\frac{\mathrm{d}^4\alpha_0}{\mathrm{d}z^4} - \left(2k^2 + \gamma - \frac{\mathrm{R}}{\mathrm{M}}\right)\frac{\mathrm{d}^2\alpha_0}{\mathrm{d}z^2}\right]\Bigg|_{z=1} = 0, \tag{16}$$

$$\left[\frac{\mathrm{d}^5\alpha_0}{\mathrm{d}z^5} - \left(2k^2 + \gamma\right)\frac{\mathrm{d}^3\alpha_0}{\mathrm{d}z^3} + k^2\left(k^2 + \gamma\right)\frac{\mathrm{d}\alpha_0}{\mathrm{d}z}\right]\Bigg|_{z=1} = 0.$$

The form of the stream function $\psi(x, z, t) = \alpha_0(z)\cos(kx)\exp(\gamma t)$ implies that the velocity perturbation increases for $\gamma > 0$, decays for $\gamma < 0$, and perturbations are stationary for $\gamma = 0$. We should find the range of Rayleigh numbers (or light intensity) and the wave numbers of the interference pattern, in which regular convective structures are stable. For this purpose, we seek the solution for a neutral perturbation $\tilde{\alpha}_0 = \alpha_0^{\gamma=0}(z)$ in the form $\tilde{\alpha}_0 \sim \exp(\delta z)$. In this case, Eqn (15) leads to

$$\delta^6 - 3k^2\delta^4 + 3k^4\delta^2 - \left(k^6 + \frac{1}{2}\mathrm{R}k^2\right) = 0. \tag{17}$$

This equation has six solutions:

$$\begin{aligned} &\delta_1 = f(k, \mathrm{R}), \quad \sigma_2 = -f(k, \mathrm{R}), \quad \delta_3 = a(k, \mathrm{R}) + \mathrm{i}b(k, \mathrm{R}), \\ &\delta_4 = -a(k, \mathrm{R}) - \mathrm{i}b(k, \mathrm{R}), \quad \delta_5 = a(k, \mathrm{R}) - \mathrm{i}b(k, \mathrm{R}), \\ &\delta_6 = -a(k, \mathrm{R}) + \mathrm{i}b(k, \mathrm{R}), \end{aligned} \tag{18}$$

where $f(k,\mathrm{R})$, $a(k,\mathrm{R})$, and $b(k,\mathrm{R})$ are certain functions of the wave number and the Rayleigh number. It can easily be shown that

$$\begin{aligned} \tilde{\alpha}_0 = {} & c_1\exp(fz) + c_2\exp(-fz) + c_3\exp(az)\cos(bz) \\ & + c_4\exp(az)\sin(bz) + c_5\exp(-az)\cos(bz) \\ & + c_6\exp(-az)\sin(bz). \end{aligned} \tag{19}$$

Here, $c_1 - c_6$ are the constants that should be determined from the boundary conditions (16). Thus, we obtain a system of algebraic equations for constants $c_1 - c_6$:

$$a_{ij}c_j = 0, \tag{20}$$

where $a_{ij} = a_{ij}(k, \mathrm{R})$ $(i,\ j = 1 - 6)$ are some functions constructed on the basis of the functions $f(k, \mathrm{R})$, $a(k, \mathrm{R})$ and $b(k, \mathrm{R})$. The system of equations has nontrivial solutions only if the determinant of the matrix a_{ij} is equal to zero. We use this condition to determine the required region of stability for system (20) in the form of the function $\mathrm{R} = \mathrm{R}(k)$.

5. Experimental results of excitation of convective flows

We used in our experiments horizontal cells with isotropic liquid (NLC 5TsV and MBBA) (see Fig. 1). The upper boundary of the cells was open, and a homotropic boundary condition was specified on the lower substrate of the cell with the NLC. The cells were placed between crossed polarisers and illuminated in two ways. For thin

cells, two beams from a 1.06-μm Nd^{3+} : YAG laser were incident on the NLC at small angles so that the angle between them was 2×10^{-2} rad. Thick cells were illuminated with the help of an incandescent lamp whose power was varied from zero to 200 W. In order to obtain a periodic intensity distribution, an absorption-transmission grating with a period $\Lambda \sim 2$ mm was mounted between the condenser and the cell. The temperature at the lower boundary of the cell was maintained constant (293 ± 0.3 K) with the help of circulating water from a controlled thermostat. The upper (free) boundary of the liquid was in contact with air at room temperature (293 K). Hydrodynamic motions of the NLC were observed through a microscope equipped with a photographic camera. Hydrodynamic motions were visualised by adding aluminium powder with the weight concentration 10^{-3} % to the liquid. We used 5TsB and MBBA NLCs into which a specially selected dye was added to provide the strong optical absorption of this complex ($a \sim 50$ cm^{-1} for $\lambda \sim 500$ nm). When necessary, the cell was additionally illuminated from above by radiation from a $\sim$ 3-mW He – Ne laser.

The exposure of the sample to radiation with spatially periodic intensity distribution resulted in hydrodynamic motions, which could be clearly seen through the microscope. Under certain experimental conditions (depending on intensity I_0 and ratio $2L/\Lambda$), such hydrodynamic motions are transformed into convective motions with a regular roller structure. These regular convective motions lead to a periodic distribution of the NLC director, which could be clearly seen through a polarisation microscope. After the removal of the grating (i.e., after the instantaneous replacement of the periodic intensity distribution by a uniform distribution), the periodic distribution of the director persisted for a certain time and then gradually disappeared. This is associated with the disappearance of the roller structure of convective motions (as can be seen clearly through the microscope). The period of the director distribution is equal to half the period of intensity distribution of incident light. The period of hydrodynamic motions coincided with the period of the intensity distribution.

Our observations proved that the roller structure was formed most clearly and rapidly when the layer thickness L was equal to half the period of the intensity distribution. For $L \leqslant 0.5$ mm, the periodic structure of the director distribution was formed almost instantaneously. When the grating was set in motion in the direction of the x axis for such thicknesses, the particles located on the surface of the liquid crystal were drawn in the same direction. This indicates that the dominating mechanism of the emergence of regular convective instability in this case is the action of surface forces (due to the temperature dependence of the surface tension coefficient). For $L \geqslant 0.75$ mm, such surface phenomena were not observed, the regular convective structure was apparently formed mainly due to bulk forces (due to the temperature dependence of the liquid crystal density), while regular convective movements (roller structure) became chaotic for $L \geqslant 1.75$ mm.

In our experiments, we measured the time-averaged maximum velocity component $v_x^{\max}$ of convective flows. Fig. 3 shows the dependence of $v_x^{\max}$ on the thickness of the layer of a liquid crystal for different average intensities I_0 of incident radiation. One can see that $v_x^{\max}$ has a maximum at $L \sim 1$ mm, i.e., at $L \sim \Lambda/2$. The asterisks on the curves

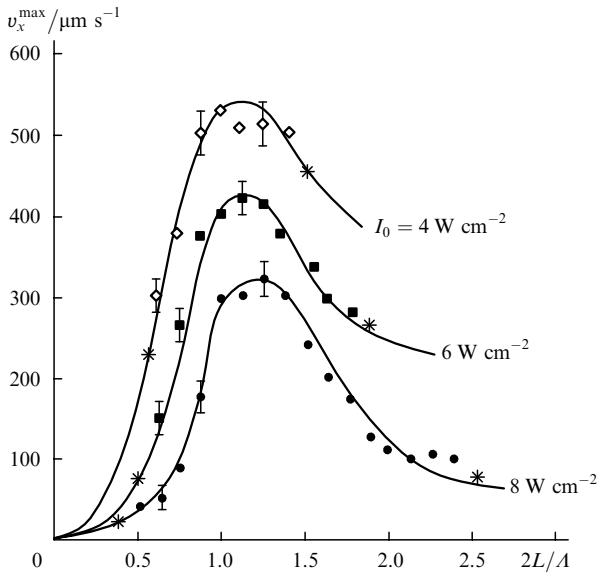

Figure 3. Time-averaged maximum velocity component $v_x^{\max}$ of convective motions as a function of the layer thickness of a liquid crystal for different intensities I_0 of incident radiation.

correspond to maximal and minimal thicknesses of the layer, between which regular convective motions of the roller type exist for the given intensity of incident radiation. We also studied the time evolution of the emerging convective motions. Although a quantitative analysis is difficult (in view of subjective perception of patterns observed through the microscope), we can assume that convective motions are stabilised 150 – 200 s after the beginning of irradiation. It can be stated that the time of stabilisation of convection decreases as L approaches $\Lambda/2$ (when $L \geqslant 0.5$ cm). A considerable decrease in this time is also observed upon an increase in the intensity of incident radiation. Fig. 4 shows the intensity dependence of $v_x^{\max}$ for $L \sim 1$ mm and $\Lambda = 2$ mm. This dependence is approximately linear to within the experimental error, which is in accord with the theoretical results.

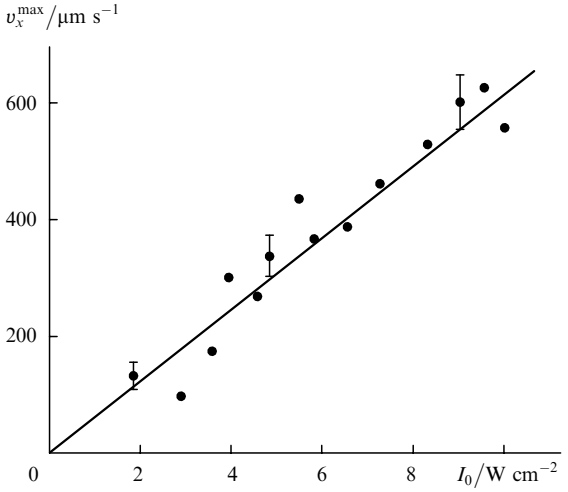

Figure 4. Experimental (circles) and theoretical (straight line) dependences of the x component of velocity on the light intensity I_0 for $L = 1$ mm and $\Lambda = 2$ mm.

For very small and very large parameters $2L/\Lambda$ and light intensity, convective roller structures become unstable. In this case, secondary thermal instabilities come into play. The experimentally observed stability regions for regular convective cells are shown on the phase diagram in Fig. 5. The dashed curves correspond to theoretical calculations. The dot-and-dash curve separates the isotropic (above the curve) and nematic (below the curve) phases of the liquid crystal. The local maximum on the dot-and-dash curve indicates that convective motions hamper the phase transition of the NLC into the isotropic phase due to efficient heat transfer for thicknesses $L \sim \Lambda/2$.

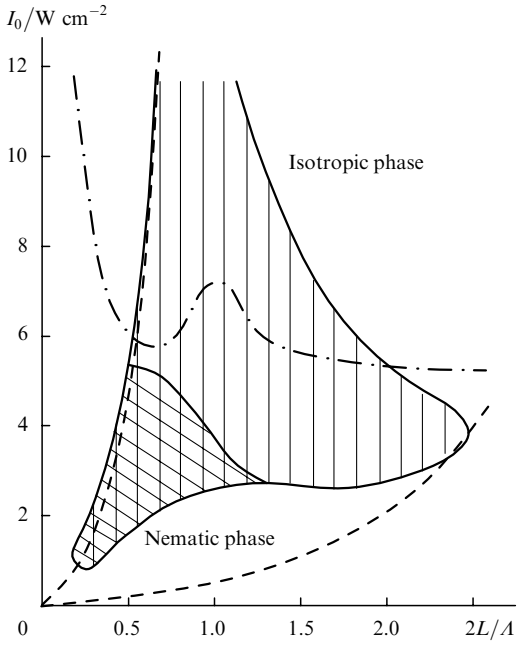

Figure 5. Phase diagram of stability of regular roller convective motions and surface hydrodynamic waves. Dashed curves correspond to theoretical calculations.

6. Observation of hydrodynamic surface waves

Because the upper surface of the liquid layer is open, it is deformed during convective motions (because the z component of velocity is nonzero on the free surface). If the interfering beams have shifted frequencies or if the grating moves at velocity W, a running pattern of the intensity distribution will be observed. Convective motions and deformation of the surface result in the emergence of gravity and capillary surface waves induced by light. The stability region for photoinduced hydrodynamic waves is shown on the phase plane (Fig. 5, doubly hatched region).

The experimental setup shown schematically in Fig. 6 was assembled to study the perturbation of the free surface of a liquid. It is well known that most optical surfaces are controlled with the help of test glasses. However, this method presumes direct contact between the standard surface and the surface being controlled, which is inadmissible in the present case. The perturbation of the liquid surface by a contactless method was investigated experimentally on a Fizeau laser interferometer [19]. A variable-width diaphragm (*3*) located in the focal plane of objective (*4*) is illuminated by monochromatic radiation emitted by a

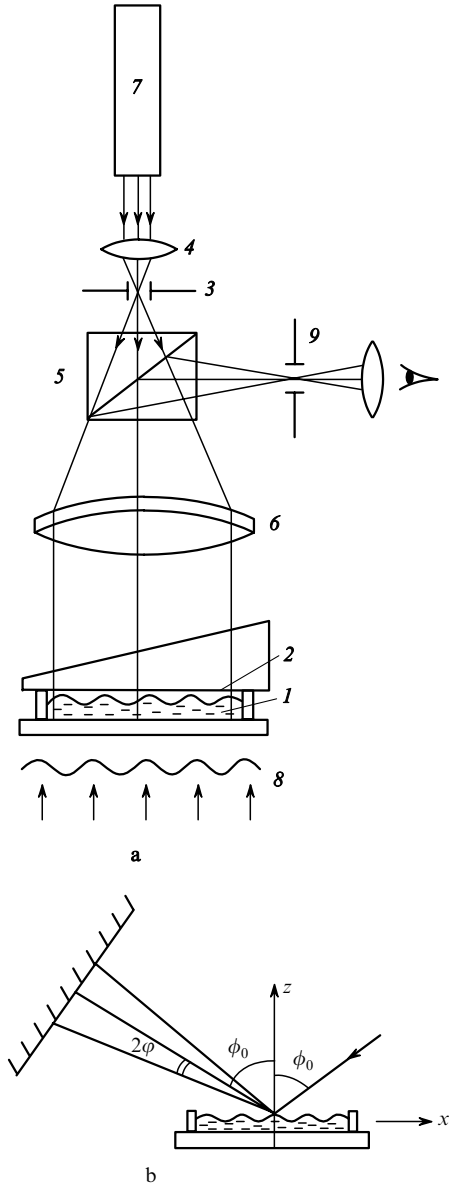

Figure 6. (a) Schematic of interferometer for observing equal-thickness fringes and (b) diagram of the experiment explaining the method of measurement of the amplitude of surface liquid vibrations: (*1*) liquid or liquid crystal under study; (*2*) standard surface; (*3*) diaphragm; (*4*) lens; (*5*) beamsplitter; (*6*) objective; (*7*) He–Ne laser; (*8*) incident spatially modulated wave; (*9*) output diaphragm.

0.63-μm He–Ne laser. The beams passing through the diaphragm and a beamsplitter (*5*) are directed to objective (*6*) forming a parallel beam incident on a wedge standard plate (*2*) and on the surface of a liquid or liquid crystal (*1*). The beams reflected from the surfaces of the liquid and the sample produce interference fringes reproducing the relief of the liquid surface being investigated. The wedge shape of the standard plate is required for deflecting the beams reflected by the upper (nonworking) surface, which may fall on the orifice of the output diaphragm (*9*) and reduce the contrast of fringes. The amplitude ξ of the surface perturbation is related to the path difference Δ of the beams by the expression

$$\Delta = 2\xi \cos\phi_0 + \frac{\lambda}{2},$$

where ϕ_0 is the angle of incidence of the beam. For $\phi_0 \approx 0$, we obtain

$$\xi = \frac{m\lambda}{2} + \frac{\lambda}{4},$$

where m is the maximal interference order within a period of the intensity distribution of exciting radiation (*8*).

Thermocapillary waves on the liquid surface were also investigated with the help of a narrow (diameter ~ 0.1 mm) He–Ne laser beam reflected from this surface. Fig. 6b shows schematically the experimental setup explaining the measuring method for the amplitude of liquid surface vibrations.

Let a sinusoidal surface wave propagate over the liquid surface. Then, the perturbation of the free surface of the liquid can be described by the equation

$$z = \xi \sin\left(\frac{2\pi}{\Lambda}x - \omega t\right), \tag{21}$$

where Λ is the wavelength of the surface wave and ω is its cyclic frequency. In this case, the maximum deflection of the reflected beam from the unperturbed direction (angle 2φ) is related to the wave amplitude ξ by the expression

$$\xi = \frac{\varphi\Lambda}{2\pi}. \tag{22}$$

In our experiments, we used a cell filled either with an isotropic liquid (diffuse oil), or with a NLC (MBBA) with a single (upper) free surface. A homotropic boundary condition was specified at the lower boundary (in the case of NLC). Such a cell was illuminated from below by an incandescent lamp whose power was varied from zero to 200 W. In order to obtain a periodic intensity distribution, a grating with period $\Lambda \approx 2$ mm was mounted between the condenser and the cell. The temperature at the lower boundary of the cell was maintained constant (293 ± 0.3 K) with the help of circulating water from a controlled thermostat. The upper free boundary of the liquid was in contact with air at room temperature (~ 293 K).

When radiation with the spatially periodic intensity distribution acted on the sample, the interference pattern in the form of equal-thickness fringes in the direction perpendicular to the wave vector of the grating was formed in the field of vision of the interferometer. These fringes indicate that the liquid surface was deformed. It acquired indentations and protrusions corresponding to the maxima and minima in the intensity distribution of the exciting radiation. Fig. 7a shows the dependence of the coordinate z of the liquid surface on the coordinate x for the sample exposed to radiation with a spatially periodic intensity distribution (the x axis is directed along the wave vector of the grating, and the plane $z = 0$ corresponds to the unperturbed free horizontal surface of the liquid). The intensity at the maximum of the distribution of exciting radiation is $I_0 = 8$ W cm^{-2}. The maxima of z for $x = \pm 1$ mm in the intensity distribution of exciting radiation corresponded to the minima; i.e., indentations were formed in the illuminated regions of the surface. Experiments show that the amplitude ξ of the surface perturbation depends on the intensity in the region 2 W cm^{-2} $\leqslant I_0 \leqslant 8$ W cm^{-2} almost linearly within the experimental error (Fig. 7b).

If the periodic structure of the intensity distribution was set in motion in the direction of the wave vector of the

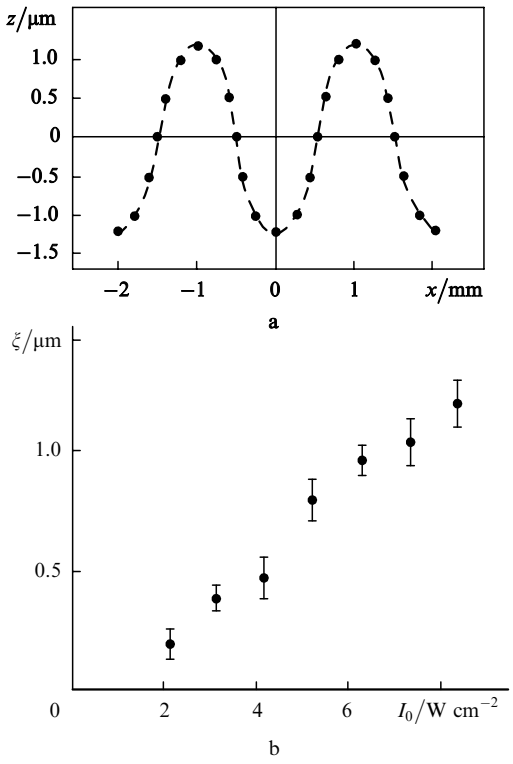

Figure 7. Dependences of the coordinate z of the liquid surface of the sample on the coordinate x under the action of radiation with a spatially periodic intensity distribution (a) and of the amplitude ξ of the surface perturbation on the intensity I_0 (b).

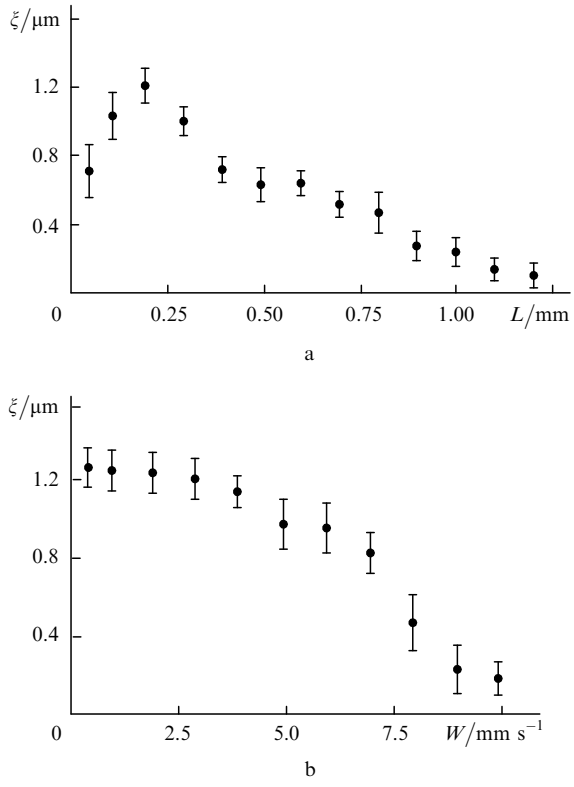

Figure 8. Dependences of the surface wave amplitude on the liquid layer thickness for the velocity $W \approx 0.1$ mm s^{-1} of the grating and the intensity $I_0 \approx 8$ W cm^{-2} (a), and on the grating velocity for $I_0 \approx 8$ W cm^{-2} and the layer thickness $L \approx 0.2$ mm (b).

grating (in the direction of the x axis), a surface wave propagating in the direction of motion of the grating was generated on the liquid surface. The velocity of this wave corresponded to the velocity $W \leqslant 10$ mm s^{-1} of the grating. For a constant intensity of incident radiation, the amplitude of this wave depended on the layer thickness and on the velocity of the grating. Fig. 8a shows the dependence of the amplitude of the surface wave on the liquid layer thickness. A typical feature of this dependence is the existence of a maximum. As the layer thickness increases, the amplitude of thermocapillary waves decreases, indicating that the contribution of the gravitational mechanism (Rayleigh – Benard convection) dominates in convection. A decrease in the amplitude of capillary waves upon a decrease in the layer thickness $L \leqslant 0.1$ mm) is apparently associated with the interaction of 'surface' molecules of the liquid with the solid substrate. The reasons for such a dependence $\xi(L)$ for small L are not completely clear and require additional experimental investigations. In particular, a considerable advance in this direction can be achieved in experiments with solid substrates.

Fig. 8b shows the dependence of the amplitude of thermocapillary waves on the grating velocity (on the velocity of a thermocapillary wave) for a constant intensity I_0 of exciting radiation. One can see that the amplitude of capillary waves depends on the velocity only slightly for not very high grating velocities $W \leqslant 4$ mm s^{-1}. For $W \geqslant 5$ mm s^{-1}, a further increase in the velocity leads to a decrease in the amplitude of capillary waves. The velocity for which the amplitude of capillary waves decreases by half is determined by the intensity of exciting light (Fig. 9).

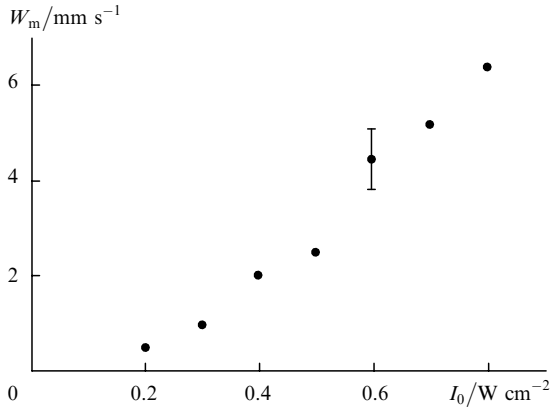

Figure 9. Velocity W_m of the grating at which the amplitude of capillary waves decreases by half as a function of the intensity I_0 of exciting radiation.

7. Discussion and conclusions

We have demonstrated theoretically and experimentally the possibility of exciting regular convective motions and surface gravitational and thermocapillary waves in isotropic liquids and liquid crystals. These effects are induced by light with a spatially periodic structure of the intensity. The hydrodynamic effects excited by light are interesting in view of the possibility to induce roller structures with desirable dislocations. The latter can be ensured by the interference of a plane light wave with another wave with a wave front dislocation. Ring-type roller structures can be produced upon the interference of a plane light wave with a wave having a conical front. The interference of three, four, and larger number of waves makes it possible to obtain cells with hexagonal, cubic, and other structures; in this case, defects can be purposefully introduced into such structures. In addition, it can be expected that, when the threshold is exceeded slightly, the light interference pattern may 'impose' its own period and phase on the steady-state pattern of rollers or cells. In our opinion, such a possibility of controlling spatial structures is quite interesting not only for liquid crystals, but also for any systems displaying instability with a finite wave number 1 cm$^{-1} \leqslant K \leqslant 10^5$ cm^{-1} of the grating in the transverse plane.

As for surface hydrodynamic waves excited by light, it is important that the wavelength, frequency, and amplitude of these waves can be controlled easily with the help of extrinsic parameters such as the frequency shift, intensities, and angles of incidence of light beams. The existence of several control parameters suggests manifestations of various excitations modes for surface waves, accompanied by bifurcation and hysteresis behaviour.

We also proved that for high and low intensities of light and the ratios of the period of the interference pattern to the cell thickness, the two-dimensional roller structure becomes unstable and is gradually transformed into a chaotic state. Because white noise enhancement in conventional experiments on turbulence masks qualitative difference in turbulent flows in various regions of extrinsic parameters, the experiments with controllable excitation are of special importance. We believe that the experiments described by us here may serve as a model in the above-mentioned sense for solving the turbulence problem in general. By separating the properties of discrete effects from the properties of stochastic noise, we have demonstrated the importance of both effects in the case of moderately turbulent convection in the general case. Moreover, the results described here together with the evidence of discrete transitions in turbulent heat transfer suggest that both effects are comparable in significance in the general case of turbulence. While convection can be studied by comparatively simple experimental methods, new methods may demonstrate qualitatively the interaction of two elements of turbulent flow in other cases of turbulence.

Acknowledgements. This work was partially supported by the CRDF Grant No. AR2-2302-UE-02.

References

1. Gershuni G.Z., Zhukhovitskii E.M. *Konvektivnaya ustoichivost' neszhimaemoi zhidkosti* (Convective Stability of an Incompressible Liquid) (Moscow: Nauka, 1972).
2. Jaluria Y. *Natural Convection* (Oxford: Pergamon Press, 1980; Moscow: Mir, 1983).
3. Getling A.V. *Konvektsiya Releya – Benara* (Rayleigh – Benard Convection) (Moscow: Editorial URSS, 1999).
4. Benard H. *Rev. Gen. Sci. Pure Appl.*, **11**, 1261 (1900); *Ann. Chem. Phys.*, **23**, 62 (1901).
5. Koschmieder E.L. *Adv. Chem. Phys.*, **26**, 177 (1974); Normand C., Pomeau Y., Velarde M.G. *Rev. Mod. Phys.*, **49**, 581 (1977); *Proc. XVII Intern. Solvay Conf.* Ed. by G. Nicolis, G. Dewel, J.W. Turner (New York: Wiley, 1981) p. 168; in *Hydrodynamic Instabilities and the Transition to Turbulence*. Ed. by H.L. Swinney, J.P. Gollub (Berlin: Springer, 1981) p. 97; in *Fluid Mechanics of Astrophysics and Geophysics*. Ed. by W.R. Peltier (New York: Gordon and Breach, 1989) Vol. 4.

6. Dubois-Violette E., Durand G., Guyon E., Manneville P., Pieranski P., in *Solid State Physics*. Ed. by L. Liebert (New York: Academic, 1978, suppl. 14); Barratt P.J. *Liq. Cryst*., **4**, 223 (1989); Kramer L., Pesch W. *Annu. Rev. Fluid Mech*., **27**, 515 (1995); Ahlers G., in *Pattern Formation in Liquid Crystals*. Ed. by L. Kramer, A. Buka (Berlin: Springer, 1996).
7. Dubois-Violette E., Gabay M. *J. Physique*, **43**, 1305 (1982).
8. Salan J., Guyon E. *J. Fluid Mech*., **126**, 13 (1983).
9. Thomas L., Pesch W., Ahlers G. *Phys. Rev. E*, **58**, 5885 (1998).
10. Gondret P., Ern P., Meignin L., Rabaud M. *Phys. Rev. Lett*., **82**, 1442 (1999).
11. Bugaev A.A., Lukoshin V.A., Urpin V.A., Yakovlev D.G. *Zh. Tekh. Fiz*., **58**, 908 (1988).
12. Viznyuk S.A., Sukhodul'skii A.T. *Zh. Tekh. Fiz*., **58**, 1000 (1988).
13. Bazhenov V.Yu., Vasnetsov M.V., Soskin M.S., Taranenko V.V. *Pis'ma Zh. Tekh. Fiz*., **49**, 330 (1989).
14. Akopyan R.S., Zel'dovich B.Ya. *Pis'ma Zh. Tekh. Fiz*., **49**, 330 (1989).
15. Akopyan R.S., Zel'dovich B.Ya., Tabiryan N.V. *Optika I Spektros*., **65**, 1082 (1988).
16. Dronyan V.E., Galstyan T.V., Alaverdyan R.B., Arakelyan S.M., Chilingaryan Yu.S. *Zh. Eksp. Teor. Fiz*., **103**, 1270 (1993).
17. Akopyan R.S., Zel'dovich B.Ya. *Mekh. Zhidk. Gaza*, **5**, 47 (1985).
18. Akopyan R.S., Khosrovyan G.R. *Zh. Tekh. Fiz*., **61** (11), 116 (1991).
19. Born M., Wolf E. *Principles of Optics* (Oxford: Pergamon press, 1969; Moscow: Nauka, 1970).